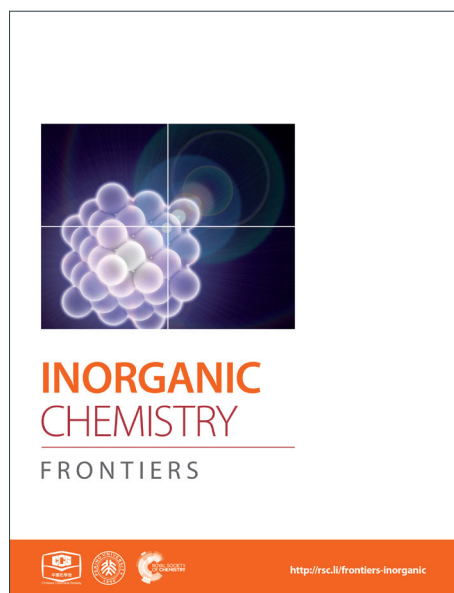
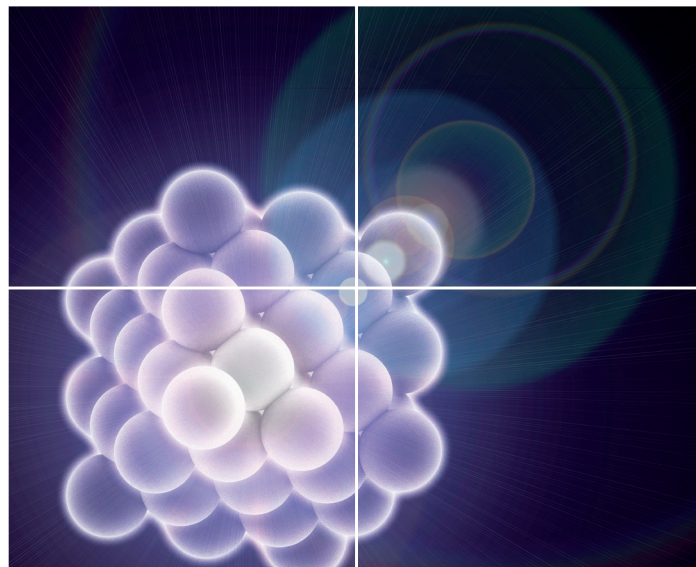


INORGANIC CHEMISTRY

FRONTIERS

Accepted Manuscript



This is an *Accepted Manuscript*, which has been through the Royal Society of Chemistry peer review process and has been accepted for publication.

Accepted Manuscripts are published online shortly after acceptance, before technical editing, formatting and proof reading. Using this free service, authors can make their results available to the community, in citable form, before we publish the edited article. We will replace this *Accepted Manuscript* with the edited and formatted *Advance Article* as soon as it is available.

You can find more information about *Accepted Manuscripts* in the [Information for Authors](#).

Please note that technical editing may introduce minor changes to the text and/or graphics, which may alter content. The journal's standard [Terms & Conditions](#) and the [Ethical guidelines](#) still apply. In no event shall the Royal Society of Chemistry be held responsible for any errors or omissions in this *Accepted Manuscript* or any consequences arising from the use of any information it contains.

ARTICLE

Effect of the Single and Double Chain Surfactant–Cobalt(III) Complexes on Their Hydrophobicity, Micelle Formation, Interaction with Serum Albumins and Antibacterial Activities

Cite this: DOI: 10.1039/x0xx00000x

Received 00th January 2012,

Accepted 00th January 2012

DOI: 10.1039/x0xx00000x

www.rsc.org/

Selvakumar Veeralakshmi,^a Selvan Nehru,^a Sankaralingam Arunachalam,^{*a} Ponnuchamy Kumar^b and Munisamy Govindaraju^b

To develop the surfactant based metallodrugs, it is important to know a correlation about the role of tail part of surfactant metal complexes on their hydrophobicity, micellization behaviour, interaction with biomacromolecules and cell penetration. Here, we have taken a new series of single and double chain surfactant–cobalt(III) complexes with alkylamine ligand of different chain length, [Co(dien)(DA)Cl₂](ClO₄) (1), [Co(dien)(HA)Cl₂](ClO₄) (2), [Co(dien)(DA)₂Cl](ClO₄)₂ (3) and [Co(dien)(HA)₂Cl](ClO₄)₂ (4), where dien = diethylenetriamine, DA = dodecylamine and HA = hexadecylamine. The structure of the complexes were characterised by elemental analysis, NMR, ESI-MS, UV–visible and FTIR techniques. In addition, the average size distribution and morphology of self-assembled surfactant–cobalt(III) complexes were examined by DLS and SEM, respectively. The hydrophobicity, critical micelle concentration (CMC) values, thermodynamics of micellization (ΔG_m° , ΔH_m° and ΔS_m°) and the nature of interaction of these complexes with bovine and human serum albumins (BSA/HSA) were evaluated. The obtained CMC values were in the order of complexes 1 > 2 > 3 > 4, indicating that double chain system have lower CMC values compared to single chain system due to increase in the hydrophobicity of alkyl amine ligands. The thermodynamics of micellization resulted that the process is spontaneous, exothermic and entropy driven. The interaction of complexes 1–4 with serum albumins indicated that the quenching process follows static mechanism, and their extent of quenching and binding parameters were in the order of complexes 1 < 2 < 3 < 4. Interestingly, on increasing temperature, protein–complex stability were decreased in case of single chain system, whereas those increased in the case of double chain systems, probably due to the involvement of electrostatic and hydrophobic interactions, respectively. This was further supported by the thermodynamics of protein interaction and synchronous fluorescence studies. Moreover, the results from UV–visible, synchronous and circular dichroism (CD) showed that occurrence of conformational and some micro environmental changes in BSA/HSA. It is also noted that BSA has more binding affinity with surfactant metal complexes compared to HSA. Furthermore, antimicrobial effects of these complexes were investigated by disk diffusion method; complex 4 have better antimicrobial activity due to ease of bacterial cell penetration by more hydrophobic in nature.

INTRODUCTION

Designing effective metallodrugs with reduced side effects against human diseases is an active area of research, and the structural modification of metallodrugs can alter their affinity with biomacromolecules such as nucleic acids, proteins, etc., In these aspects of drug designing, some of the issues like solubility, transfection efficiency, targeted delivery, etc. may enter as practical problems. To overcome these problems, drug carriers like surfactants, liposomes, vesicles, cationic polymers

^aSchool of Chemistry, Bharathidasan University, Tiruchirappalli 620024, Tamil Nadu, India.

E-mail: arunasurf@yahoo.com; Tel.: +91-431-2407053, Fax: +91-431-2407043/2407045.

^bDepartment of Environmental Biotechnology, School of Environmental Sciences, Bharathidasan University, Tiruchirappalli 620024, Tamil Nadu, India.

♣ Electronic supplementary information (ESI) available.

and dendrimers were employed for efficient drug delivery. In this pipeline, metallosurfactants have a distinctive place in designing metallo drugs. During drug designing, one of the factors, hydrophobicity of metal complexes, plays a major role in penetration of cell membrane to precede cell death.¹

Surfactant metal complexes are a new class of coordination compounds in which metal containing coordination sphere acts as hydrophilic head group, whereas long alkyl chain containing ligand acts as hydrophobic tail group. Especially, such surfactant metal complexes are rare compared to conventional surfactants, but they have very important applications in diverse subject research areas such as magnetic resonance imaging,^{2,3} templating of mesoporous materials,⁴ thin film-opto electronics,⁵ drug delivery⁶ and homogeneous catalysis.^{7,8} Several studies are available about the effect of head and tail groups on the micellization behavior, but those are not yet clear in case of surfactant metal complexes. To develop the surfactant based metallo drugs, it is very important to know about how the surfactant metal complexes should affect their hydrophobicity, critical micelle concentration, and their impacts on interaction with biomacromolecules such as proteins, nucleic acids, and biological activities such as antitumor, antimicrobial, antioxidant and anti-inflammatory.

Particularly, research on cobalt-based pharmaceuticals have attracted to develop promising applications such as potential hypoxia-activated pro-drugs, chaperones of bioactive ligands to target tumors through bio-reductive activation, higher inhibition of chymotrypsin-like activity in purified proteasomes as well as improved apoptotic induction in PC-3 cancer cells, artificial proteases, HIV protease inhibitor⁹ and clinically reached cobalt(III) schiffbase complex, Doxovir.^{10,11}

Protein-drug interactions are closely related to the drug efficiency in the treatment of diseases, because of the absorption, transportation, distribution and metabolism of drugs strongly depend on their binding properties.¹² Generally, the strong binding with protein decreases the concentrations of free drug in plasma, whereas weak binding leads to shorter lifetime or poor distribution of drugs. Moreover, the investigation of binding of the drugs to serum albumins has provided a great toxicological and medical importance, and it may afford key information to rational drug design.¹³⁻¹⁵ Even though many surfactants exhibit very good antibacterial activities, the impact of protein binding affinity of metallosurfactants on antibacterial activities isn't still clear.

Interaction of proteins with surfactants mainly depends on surfactant features like size, charge, chain length, hydrophobicity, concentration, etc. Several reports have been investigated on the interaction of proteins with conventional surfactants but those with surfactant metal complexes are limited. Thus, the present study has been focused on how the single and double chain surfactant-cobalt(III) complexes (**Figure 1.**) affect their hydrophobicity, CMC and its thermodynamic parameters, and the interaction with BSA and HSA. To extend our study we have also performed antibacterial activity by disk diffusion method using some human pathogenic strains.

RESULTS AND DISCUSSION

Characterization of surfactant-cobalt(III) complexes

The single and double chain surfactant-cobalt(III) complexes were synthesised from $[\text{Co}(\text{dien})\text{Cl}_3]$ by ligand substitution method in which one or two labile chloride ligands were replaced by one or two amine groups of the alkylamine

ligands (**Scheme 1**). The UV-visible absorption spectra of surfactant-cobalt(III) complexes clearly show an intense band around 213–219 nm due to $\text{N}(\sigma) \rightarrow \text{Co}(\text{III})$ charge transfer and a band around 511–522 nm due to d-d transitions.¹⁶ The IR spectra can afford the characteristic vibrational frequencies for the formation of surfactant-cobalt(III) complexes. The precursor complex, $[\text{Co}(\text{dien})\text{Cl}_3]$ shows N–H, C–H symmetric and asymmetric stretching vibrational bands around 3615, 2852 and 2921 cm^{-1} were red shifted to 3439, 2849 and 2917 cm^{-1} after coordination with alkylamine in the surfactant-cobalt(III) complexes, respectively (**Figure S1**). These shifts can be explained by the fact that nitrogen atom of alkyl amine ligand donate a pair of electrons to the cobalt centre forming a coordinate bond. The band observed around 1113 cm^{-1} can be assigned to perchlorate ionic species; this means that the counter ion was not involved in the coordination to cobalt. Furthermore, the bands around 627 and 1088 cm^{-1} can be attributed to the (C–N) and (C–N) stretching vibrations of surfactant-cobalt(III) complexes.¹⁷ The ¹H NMR spectra were also resulted the corroboration of structure of surfactant-cobalt(III) complexes. The methylene protons of the alkyl amine chains and dien ligands were appeared in the region of 0.99–3.08 ppm for complexes **1–4** (**Figure S2**). It is also noted a typical triplet signal at 0.84 ppm correspond to the terminal methyl group of the long aliphatic alkyl amine chain. The N–H protons were appeared as broad peaks in the region of 4.60–8.00 ppm. The ¹³C NMR spectra of complexes **1–4** gave signals in the region of 22.07–31.21 ppm due to the merging of methylene carbon signals of alkyl amine chain and dien ligands. Furthermore, a signal around 13.87 ppm was observed for terminal methyl carbon. ESI-MS spectra of complexes **1–4** showed molecular ion peaks at 417.32, 472.89, 283.08 and 339.17, respectively.

Morphology and size distribution of self-assembled surfactant-cobalt(III) complexes

The average hydrodynamic size and surface morphology of the self-assembled surfactant-cobalt(III) complexes were examined by DLS and SEM, respectively.¹⁸⁻²⁰ SEM images and size distribution histogram plots for self-assembled surfactant-cobalt(III) complexes are presented in **Figure 2(a) and 2(b)**. The SEM results show that the self-assembled surfactant-cobalt(III) complexes are spherical and rod like shape, and their size distribution for the complexes **1–4** as 58.55, 97.79, 108.30 and 120.16 nm, respectively. The rod like morphology²¹ were preferably formed on increasing hydrophobicity of surfactant-cobalt(III) complexes. As shown from **Figure S3**, self-assembled surfactant-cobalt(III) complexes exhibit monodisperse and narrow size distribution with an average hydrodynamic diameter for the complexes **1–4** as 117.9, 136.3, 151.0 and 188.5 nm, respectively with polydispersity index (PDI = 1.00).²¹ The obtained size distribution from DLS measurements are larger than that of SEM measurements, may be due to experimental conditions.¹⁹

Determination of partition coefficient

Hydrophobicity of surfactant metal complexes is an important parameter to analyse penetration behaviour across the cell membrane, and is compared in terms of partition coefficient (log P).²² Here, the surfactant-cobalt(III) complexes are likely to differ in their hydrophobicity due to the variation in the single and double chain system of different chain length. Based on the concentration of surfactant-cobalt(III) complexes

distributed in the biphasic system (n-octanol/water), partition coefficients were calculated by the following equation.

$$\log P = \log \left[\frac{[\text{complex}]_{\text{octanol}}}{[\text{complex}]_{\text{water}}} \right] \dots \dots \dots (1)$$

The calculated values of log P for complexes **1–4** are –1.23, –1.03, –0.94 and –0.86 respectively, and are in the order of **1 < 2 < 3 < 4**. That is the hydrophobicity of double chain surfactant–cobalt(III) complexes are higher than that of respective single chain surfactant–cobalt(III) complexes (**1, 2 < 3, 4**). However, within the single or double chain surfactant–cobalt(III) complexes, complexes with longer alkyl chain length have higher hydrophobicity than complexes with shorter alkyl chain length (**1 < 2; 3 < 4**).

Critical micelle concentration

The surfactant metal complexes tend to aggregate themselves in aqueous medium on increasing their concentration, and start to form micelles at a particular concentration called critical micelle concentration, and during which their physical properties like specific conductivity also altered, due to change in the mobility of molecules in the system. A typical change in the specific conductivity of surfactant–cobalt(III) complexes of the present study with increase of concentration at five different temperature (303, 308, 313, 318 and 323 K) were observed and the values were plotted in **Figure 3 and S4**. The obtained plots for all the surfactant–cobalt(III) complexes showed a sharp change from the pre micellar to post–micellar regions due to the reduction in the mobility of molecules by aggregation. However, CMC value gets increased with increase of temperature, due to the disturbance in the aggregation.²³

The obtained CMC values for the surfactant–cobalt(III) complexes are shown in **Table 1**, and are very low compared to most of the simple organic surfactants due to larger head group size which results reduction in the concentration of micelles.²⁴ Thus it is suggested that these surfactant–cobalt(III) complexes have more capacity to associate themselves forming micellar aggregates than ordinary synthetic organic surfactants. The order of CMC values for complex **1>2>3>4**, which clearly shows that surfactant–cobalt(III) complexes with higher alkylamine chain length as well as complexes with more number of alkylamine ligand have lower CMC values. And the double chain surfactant–cobalt(III) complexes are found to have lower CMC value than the respective single chain complexes. This is due to the increase in the hydrophobicity of tail part, tend to favour aggregation for micellization at lower concentration.

Thermodynamics of micellization

Phase separation or the equilibrium model for micelle formation was used to derive the various thermodynamic parameters of micellization by monitoring the change in the CMC with temperature. The sign and magnitude for the formation of micelles by ionic, non-ionic and zwitterionic surfactants have been reported.¹⁷ The thermodynamic parameters for the micellization by the single and double chain surfactant metal complexes are compiled in **Table 1**. Generally it is noted that micelle formation results $-\Delta G_m^\circ$, $-\Delta H_m^\circ$ and $+\Delta S_m^\circ$ values. The negative Gibbs free energy change denoted that the process of micelle formation is spontaneous and this

was gradually increase with the temperature as well as chain length and number of alkylamine ligands. In all the cases, ΔS_m° decreases with increasing temperature, this is due to head group is more hydrated than the hydrophobic tail. Whereas, ΔH_m° increases with increase in temperature, indicating the formation of micelles becomes increasingly exothermic.^{25, 26}

Interaction of surfactant–cobalt(III) complexes with serum albumins

The biophysical studies on the interaction between protein and surfactant-metal complexes can give valuable information about structural factor governing protein–drug binding behaviour. To develop efficient metalodrugs, it is important to analyse the process behind the protein–drug complex formation (i) whether drug interact with the ground state protein (static process) or with the excited state protein (dynamic process),²⁷ (ii) strength and stability of protein–drug complex, (iii) binding number of protein–drug complex formation, (iv) the nature of binding forces (electrostatic, hydrophobic, hydrogen bonding and van der Waals interaction) acting upon the protein–drug complex formation, and (v) conformational and microenvironmental changes in the protein.

UV–visible absorption studies

UV–visible absorption technique can afford the support for the above observed static process based on the changes in the absorption peaks of protein. Absorption spectrum of protein is only influenced by the complexation with quencher in the ground state (static process) rather than in the excited state (dynamic process).²⁸ The absorption spectra of BSA/HSA in the absence and presence of surfactant–cobalt(III) complexes are shown in **Figure 4 and S5**. Generally it is noticed that the addition of surfactant–cobalt(III) complexes to the protein solution results hypochromism around 210 nm responsible for α -helix contents of protein and hyperchromism around 280 nm responsible for aromatic residues of proteins. The observed hypochromism shows the occurrence of structural influence in the α -helix of protein, whereas hyperchromism shows the occurrence of alteration in the microenvironment around the aromatic acid residues probably through the extending into the aqueous environment. These changes in the absorbance of protein by the interaction with surfactant–cobalt(III) complexes can be the evidence for existence of static quenching process.

Analysis of quenching and binding parameters

To investigate quenching and binding nature of surfactant–cobalt(III) complexes with serum albumins, the emission spectra of BSA and HSA solutions were monitored in the wavelength range 290–450 nm by exciting the proteins at 280 nm, resulting a strong fluorescence emission peak at 350 nm for BSA and 346 nm for HSA due to their tryptophan residues. The changes in the emission spectra of protein with increase of surfactant–cobalt(III) complex concentration at three different temperatures (278, 293 and 308 K) were recorded and the representative fluorescence emission spectra are shown in **Figure 5**. Generally it is noticed that fluorescence emission intensities of protein is quenched regularly by addition of surfactant–cobalt(III) complexes, indicating the formation of efficient complex between protein and surfactant metal complexes.²⁹ The obtained results were analysed through

equations (4) and (5) and the values for K_{sv} , k_q , K_b and n are summarized in **Table 2**.

As all the Stern–Volmer plots are linear, it is concluded that the existence of a single type of quenching mechanism, either static or dynamic, which can be distinguished from the temperature dependence of K_{sv} and k_q values. It is known that higher temperature is likely to result in decreasing of quenching constant values for static process due to weakening of ground state complex stability, whereas, an increasing of quenching constant values for dynamic process due to the faster diffusion of the excited molecules.³⁰ Thus the increasing mannerism of the quenching constant values (K_{sv} and k_q) with respect to temperature (**Table 2**) indicating that the stimulation of dynamic quenching process upon BSA/HSA by the surfactant–cobalt(III) complexes.

However, the obtained quenching rate constant values ($k_q \approx 10^{11}$ – $10^{12} \text{ M}^{-1} \text{ s}^{-1}$) are 10–100 times higher than the maximum value possible for diffusion controlled dynamic quenching (i.e., $2.0 \times 10^{10} \text{ M}^{-1} \text{ s}^{-1}$). This observation can be explained based on the existence of special process in which surfactant–cobalt(III) complexes probably quenches the BSA/HSA via initiation of static mechanism rather than dynamic process.^{31,32}

Similarly the values of binding number per albumin molecule (n) is around 1, indicating strong and independent binding site granted by BSA/HSA to the surfactant–cobalt(III) complexes. It is also observed that the extent of binding (K_b) between protein and surfactant–cobalt(III) complexes with respect to temperature decreased for single chain system, whereas this has increased for double chain systems. This may be due to the increase of temperature diminishes the electrostatic attraction between protein and single chain surfactant–cobalt(III) complexes, thereby decreases the stability of protein–surfactant cobalt(III) complexes. However, the increase of temperature tightens the hydrophobic attraction between protein and double chain surfactant–cobalt(III) complexes, thereby increases the stability of protein–surfactant metal complexes.²⁷

Thermodynamic parameters and nature of the binding forces

In order to analyse the nature of binding forces (hydrophobic, electrostatic, hydrogen bonding and van der Waals interactions) existing between protein and surfactant–cobalt(III) complexes, the sign and magnitude of the thermodynamic parameters such as ΔG° (free energy change), ΔH° (enthalpy change), and ΔS° (entropy change) for the interaction process were calculated by using the equations 5 and 6. Ross and Subramanian³³ have studied the various models to explain the existence of principal binding forces in the protein association process using thermodynamic parameters and the results showed that, (i) both positive ΔH° and ΔS° resulted by hydrophobic forces, (ii) both negative ΔH° and ΔS° resulted by van der Waals interaction and hydrogen bond formation, and (iii) negative ΔH° and positive ΔS° resulted by electrostatic interaction. As seen from the **Table 2**, the negative free energy change values for the interaction between surfactant–cobalt(III) complexes and BSA/HSA indicate that the binding process is spontaneous. The positive ΔH° and ΔS° values indicate that hydrophobic interactions played a dominant role in the interactions between double chain surfactant–cobalt(III) complexes and BSA/HSA.³⁴ Whereas, the negative ΔH° and positive ΔS° values for the interaction between single

chain surfactant–cobalt(III) complexes and BSA/HSA indicates that the electrostatic interaction plays a major role.

Synchronous fluorescence studies

Synchronous fluorescence spectroscopy is used to monitor the microenvironmental and conformational changes around the vicinity of tryptophan (Trp) and tyrosine (Tyr) chromophores in the protein, following their extent of quenching and shift in the emission maximum by the addition of surfactant–cobalt(III) complexes. The characteristic emission for the tyrosine and tryptophan residues of the protein can be obtained by maintaining the wavelength interval ($\Delta\lambda$) as 15 and 60 nm, respectively³⁰. For the investigated concentration range, the changes in the synchronous fluorescence spectra of BSA/HSA upon increasing the concentration of surfactant–cobalt(III) complexes at $\Delta\lambda = 15$ and 60 nm are shown in **Figure 6**.

As seen from the **Figure 6**, in case of BSA, fluorescence intensity of Tyr/Trp residues is relatively more quenched than in the case of HSA which may be due to presence of more aromatic residues in BSA. It can also be noticed that surfactant–cobalt(III) complexes interact with both Tyr and Trp residues in a similar manner, indicating non-specific binding. In addition to this, there is no significant shift in the emission maximum of Tyr residues upon addition of complexes **1–4**. In contrast, an obvious red shift in the emission of Trp residues was noticed for the single chain surfactant metal complexes, which indicated that there is enhancement of polarity by the reduction of hydrophobicity. Whereas, a slight blue shift in the emission of tryptophan residues was observed for double chain surfactant metal complexes, which indicates that the polarity around the tryptophan residues was decreased by the increase of hydrophobicity due to conformational changes in BSA/HSA. From this result we can conclude that double chain surfactant–cobalt(III) complexes should have higher hydrophobic character than the single chain surfactant–cobalt(III) complexes.

Circular Dichroism spectroscopic studies

CD spectroscopy is a sensitive technique to investigate the changes in the secondary structure of protein upon interaction with metalldrugs. The far-UV CD spectra of BSA/HSA exhibit two negative bands at 208 and 222 nm, which are characteristic of the typical α -helical structure of protein and is contributed by the $n \rightarrow \pi^*$ transfer of the peptide bonds of α -helix.^{35–37} So in order to obtain an insight into the changes in the secondary structure of BSA/HSA upon interaction with surfactant–cobalt(III) complexes, the far-UV CD spectra of BSA/HSA were recorded in the absence and presence of complexes **1–4**.

As can be seen from **Figure 7**, the negative ellipticity values of BSA/HSA decreased by the addition of surfactant–cobalt(III) complexes, indicating the unfolding of peptide strands, thereby lowering of the α -helical content in the protein. The extent of decreasing the α -helical content in BSA/HSA by the complexes **1–4** is in the order of **1 < 2 < 3 < 4**, showing that the binding of surfactant–cobalt(III) complexes with BSA/HSA induces conformational changes in BSA/HSA, which may affect the physiological functions of proteins.

Based on the results present in the **Figure 7**, it is found that the percentage of change of α -helix of proteins by the complex **3** and **4** are lower than that of complex **1** and **2**, according to the hydrophobicity factors. This change in α -helix of proteins

shows a direct relationship between the length of hydrophobic tail of the surfactant–cobalt(III) complexes and protein confirmation. In order to explore the effect of additional alkyl chain of surfactant–cobalt(III) complexes on conformation of BSA/HSA, the α -helix content of single and double chain complexes were compared and it is observed that α -helix content protein has been reduced to a large extent in the presence of double chain complexes than the respective single chain complexes. This is due to the larger hydrophobicity of double chain than the single chain surfactant–cobalt(III) complexes.

Antibacterial activity

A disk diffusion assay was adopted to test the antibacterial activity of single and double chain surfactant–cobalt (III) complexes against human pathogens. The complexes exhibited good antibacterial activity against both gram–positive and gram–negative bacteria with reference to standard antibiotic drug (Ciprofloxacin). The killing effect of the complexes is in relation with the concentration of drug in a dose-dependent manner (i.e.,) higher concentration of surfactant–cobalt (III) complexes have greater killing effect than the lower concentration in all tested microorganisms. The results of the antibacterial activities of complexes at different concentrations (0, 250, 500 750, 1000 $\mu\text{g mL}^{-1}$) are summarized in **Table 3** and **Figure S6** and **S7**. We found that, *E. coli* is highly susceptible to all complexes while *K. pneumoniae* and *P. aeruginosa* is least susceptible respectively. A moderate level of susceptibility is noticed in strains such as *P. vulgaris*, *S. aureus*, *S. flexneri* and *S. typhii*. Out of the four surfactant–cobalt (III) complexes, the complex 4 possessed very good antibacterial activity against all the microbes used. In addition to this, percentage of increase (%) of bacterial inhibition between the standard (Ciprofloxacin) and complex (1–4) was also evaluated (**Table S1** and **Figure S8**). The percentage fold increase of Complex-4 was found to be 51.35 % (*E. coli*), 52.94 % (*P. vulgaris*), 67.4 % (*S. typhii*), 56.25 % (*S. flexneri*), 52.94 % (*S. aureus*) and 37.5% (*V. cholerae*) against Ciprofloxacin. On the other hand, Complex-2 displayed effective inhibition against *K. pneumoniae* (23.52 %) and Complex- 2 and 3 against *P. aeruginosa* (33.33 %) as compared to standard. The reason behind this may be mainly attributed to the hydrophobicity of complex which can penetrate cell wall inducing DNA damage.³⁸ It is also reported that, the ionic interaction between the surfactant (cationic charge) and cell membrane (anionic charge) may play a major role in diffusion of complexes into bacteria.³⁹ Meanwhile, complex of similar kind have possessed significant antibacterial activity against gram–positive and gram–negative bacteria. However, the study may require further investigation to elucidate the actual mechanism involved in the killing effect of bacterial strains.

EXPERIMENTAL SECTION

Materials

BSA (lyophilized powder, essentially fatty acid free and globulin free $\geq 99\%$), HSA (lyophilized powder, fatty acid free and globulin free $\geq 99\%$), dodecylamine, hexadecylamine were purchased from Sigma Aldrich and used as supplied. The cobaltous chloride, diethylenetriamine were obtained from Rankem, India. For micro biological studies, ingredients were purchased from HiMedia Laboratories. All other chemicals

were of analytical reagent grade, and double distilled water was used throughout the study.

General Methods

Elemental analysis (C, H, and N) were carried out at Perkin-Elmer Series II 2400 CHNS/O Elemental Analyzer. Electrospray ionisation mass spectrometry (ESI–MS) analysis was performed in the positive ion mode on a liquid chromatography–ion trap mass spectrometer (LCQ Fleet, Thermo Fisher Instruments Limited, US). Complexes 1–4 were dissolved in water, and the mass scan range was from 100 to 1000 amu. ¹H and ¹³C NMR measurements were performed on BRUKER 400 MHZ NMR spectrometer using d6–DMSO as solvent. Infrared spectra were recorded using Perkin-Elmer FT–IR spectrophotometer with samples prepared as KBr pellets. Absorption measurements were performed on Shimadzu UV–1800, UV–Vis spectrophotometer using cuvettes of 1 cm path length. Circular dichroism spectra were recorded on a JASCO–J810 spectropolarimeter with a cylindrical cuvette of 0.1 cm path length. Fluorescence experiments were carried out on a thermostatic bath coupled JASCO FP650 spectrofluorometer using a 1 cm quartz cuvette. Conductivity measurements were made with an Elico Conductivity bridge type CM 82 and dip-type cell with a cell constant of 1.0.

The surface morphology and average size distribution of self-assembled surfactant–cobalt(III) complexes were analysed by SEM on VEGA3 TESCAN at an accelerating voltage of 30 kV. A drop of aqueous solution of surfactant–cobalt(III) complex was placed on FTO plate (Agar Scientific Ltd, UK) and it was air dried at room temperature. The average hydrodynamic diameter of the surfactant–cobalt(III) complexes were measured by DLS on ZetaSizer NanoSizer 90 ZS (Malvern Instruments) equipped with He-Ne Laser. All the measurements were carried out at a wavelength of 633.8 nm and the data were analysed in an automatic mode. Measured size was presented as the average value of 20 runs, with triplicate measurements within each run. The percentage of cobalt content present in the surfactant–cobalt(III) complexes were determined spectrophotometrically by converting the complexes into $[\text{CoCl}_4]^{2-}$ whose molar absorbance coefficient is $561 \text{ M}^{-1} \text{ cm}^{-1}$ at 691 nm.⁴⁰

Synthesis of surfactant–cobalt(III) complexes

$[\text{Co}(\text{dien})\text{Cl}_3]$ was synthesised according to the reported procedure.⁴¹ To a saturated aqueous solution of $[\text{Co}(\text{dien})\text{Cl}_3]$ (3.2215 g, 0.2825 mmol), ethanolic solution of respective mole ratio of ligand, dodecylamine (2.757 mL, 0.1854 mmol for **1**; 5.514 mL, 0.3708 mmol for **3**), hexadecylamine (2.953 mL, 0.2415mmol for **2**; 5.906 mL, 0.4831 mmol for **4**) was added drop by drop over a period of 30 min. During this addition, the dark violet colour of the solution gradually became light violet and the resulting mixture was kept at room temperature for 48 h. Afterwards, a saturated solution of sodium perchlorate in very dilute perchloric acid was added to the reaction mixture. The obtained precipitate was filtered off and washed with cold ethanol followed by acetone, and dried over fused calcium chloride and stored in a vacuum desiccator.

$[\text{Co}(\text{dien})(\text{DA})\text{Cl}_2]\text{ClO}_4$ (**1**)

Violet colour solid; Yield: 78%; Anal. Calc. for $\text{C}_{16}\text{H}_{40}\text{Cl}_3\text{CoN}_4\text{O}_4$: C, 37.09; H, 7.79; N, 10.68; Co, 11.38. Found: C, 37.02; H, 7.85; N, 10.75; Co, 11.29. ESI–MS (H_2O ,

m/z): 417.32 [Co(dien)(DA)Cl₂]⁺. ¹H NMR δ_H(ppm) 7.91–7.68 (4H), 4.77 (2H), 3.06–3.01 (1H), 2.76–2.73 (2H), 2.61–2.54 (2H), 2.34–2.30 (1H), 1.52–1.49 (2H), 1.22 (22H), 0.83 (3H). ¹³C NMR (400 MHz, DMSO-d₆): δ (ppm) 16.5, 29.43, 31.37, 31.58, 33.96, 42.05. IR (KBr, cm⁻¹) γ_{max}: 626, 1089, 1148, 1638, 2849, 2917, 3443. UV-Vis in water (λ_{max}, nm) (ε/M⁻¹cm⁻¹): 213 (1888), 520 (112).

[Co(dien)(HA)Cl₂](ClO₄)₂ (2)

Light brown colour solid; Yield: 74%; Anal. Calc. for C₂₀H₄₈Cl₃CoN₄O₄: C, 41.86; H, 8.48; N, 9.79; Co, 10.27; Found: C, 41.80; H, 8.57; N, 9.83; Co, 10.11. ESI-MS (H₂O, m/z): 472.89 [Co(dien)(HA)Cl₂]⁺. ¹H NMR (400 MHz, DMSO-d₆): δ(ppm) 7.9–7.74 (3.5H), 5.00–4.77 (3.5H), 3.08–2.97 (2H), 1.53–1.49 (2H), 1.22 (30H), 0.84 (3H). ¹³C NMR (400 MHz, DMSO-d₆): δ (ppm) 13.91, 22.04, 25.71, 28.78, 31.24, 39.28. IR (KBr, cm⁻¹) γ_{max}: 629, 724, 1088, 1127, 1149, 1467, 1504, 1589, 1634, 2849, 2918, 3415. UV-Vis in water (λ_{max}, nm) (ε/M⁻¹cm⁻¹): 522 (82), 210 (1460).

[Co(dien)(DA)₂Cl](ClO₄)₂ (3)

Violet colour solid; Yield: 83%; Anal. Calc. for C₂₈H₆₇Cl₃CoN₅O₈ (Found): C, 43.84; H, 8.80; N, 9.13; Co, 7.68; Found: C, 43.90; H, 8.69; N, 9.05; Co, 7.42. ESI-MS (H₂O, m/z): 283.08 [Co(dien)(DA)₂Cl]²⁺. ¹H NMR (400 MHz, DMSO-d₆): δ(ppm) 7.61 (9H), 2.77–2.73 (4H), 1.50–1.48 (4H), 1.23 (44H), 0.84 (6H). ¹³C NMR (400 MHz, DMSO-d₆): δ (ppm) 13.86, 22.02, 26.88, 28.42, 28.84, 31.22, 39.34. IR (KBr, cm⁻¹) γ_{max}: 627, 1089, 1110, 1147, 1470, 1637, 2850, 2917, 3440. UV-Vis in water (λ_{max}, nm) (ε/M⁻¹cm⁻¹): 516 (761), 216 (1310).

[Co(dien)(HA)₂Cl](ClO₄)₂ (4)

Light brown colour solid; Yield: 85%; Anal. cald. for C₃₇H₈₇Cl₃CoN₅O₈ (Found): C, 49.63; H, 9.79; N, 7.82; Co, 6.58; Found: C, 49.56; H, 9.71; N, 7.77; Co, 6.53. ESI-MS (H₂O, m/z): 339.17 [Co(dien)(HA)₂Cl]²⁺. ¹H NMR (400 MHz, DMSO-d₆): δ(ppm) 7.54–7.52 (6H), 4.79 (3H), 2.27 (4H), 1.28 (4H), 0.99 (60H), 0.61 (6H). ¹³C NMR (400 MHz, DMSO-d₆): δ (ppm) 13.87, 22.01, 28.84, 28.95, 31.21, 39.42. IR (KBr, cm⁻¹): 628, 1087, 1116, 1146, 1470, 1633, 2850, 2918, 3439. UV-Vis in water (λ_{max}, nm) (ε/M⁻¹cm⁻¹): 681 (40), 511 (80), 219 (5160).

Partition Coefficients Determination

The hydrophobicity values of surfactant–cobalt(III) complexes (1–4) were measured by the “Shake flask” method in octanol/water phase partitions as reported earlier.⁴² Complexes (1–4) were dissolved in a mixture of water and n-octanol followed by shaken for 1 hour. The mixture was allowed to settle over a period of 30 minutes and the resulted two phases were collected separately without cross contamination of one solvent layer into another. The concentration of surfactant–cobalt(III) complexes in each phase was determined by UV-Vis absorption spectroscopy at room temperature. The results are given as the mean values obtained from three independent experiments.

Conductivity measurements

Conductivity measurements were made in a thermo stated water bath maintaining the temperature constant within ±0.1 °C, after calibrating cell constant with standard KCl solutions of known specific conductivities. Specific conductivity values for the aqueous solution of surfactant–cobalt(III) complexes having

concentration in the range of 10⁻⁶–10⁻² M⁻¹ were measured at 303, 308, 313, 318 and 323 K. Each reading was noted after thorough mixing and temperature equilibration until no significant change occurred. The CMC values were obtained by plotting specific conductance versus concentration of surfactant–cobalt(III) complex. The change in the CMC with temperature was analysed from phase separation model or equilibrium model for micelle formation.²⁵ The thermodynamic parameters were calculated as given in the **supporting information**.^{43, 44}

Interaction studies with serum albumins

Throughout protein binding studies was carried out using Tris-HCl buffer (pH = 7.4), and the concentrations of BSA and HSA were determined spectrophotometrically from the respective molar extinction coefficient of 43,800 and 36,500 M⁻¹ cm⁻¹ at 278 nm. The initial setup was made for fluorescence measurements as: excitation and emission slits were set at 5 nm and 3 nm, respectively, and scanning speed was set at 500 nm/min. The fluorescence emission spectra were recorded in the wavelength range 290–450 nm by exciting at 280 nm. UV-visible experiments were performed by keeping the concentrations of BSA/HSA (10 μM) and varying concentrations of surfactant–cobalt(III) complexes (0–90 μM), and the absorbance due to complex itself is nullified by adding in both sample and reference cells. The fluorescence quenching experiments were carried out in a manner that the concentration of protein and surfactant–cobalt(III) complexes was fixed as those used in the UV-visible studies. The synchronous fluorescence spectra were recorded with Δλ = 15 nm and Δλ = 60 nm for tyrosine and tryptophan residues respectively. In CD spectral measurements, the concentration of BSA/HSA was maintained at 2 μM. The spectra were recorded in the range of 200–270 nm with a scan rate of 200 nm/min and a response time of 4 s. Three scans were accumulated for each spectrum. By correcting the inner filter effect⁴⁵ for the interaction between surfactant–cobalt(III) complexes and BSA/HSA, quenching and binding parameters,⁴⁶⁻⁴⁹ thermodynamics of interaction^{33, 50, 51} and percentage of α-helix⁵²⁻⁵⁴ were calculated as given in the **supporting information**.

Antibacterial activity

The antibacterial activity of single and double chain surfactant–cobalt (III) complexes was tested against human pathogenic strains by disk diffusion assay.³⁸ This method is a valuable, inexpensive tool for the demonstration of antibacterial susceptibility of a particular compound by measuring its relative zone of inhibition. Bacterial cultures such as *Escherichia coli* (MTCC-1687), *Salmonella typhi* (MTCC-531), *Pseudomonas aeruginosa* (MTCC-350), *Staphylococcus aureus* (MTCC-96), *Proteus vulgaris* (MTCC-425), *Klebsiellapneumoniae* (MTCC-350), *Shigella flexneri* (MTCC-1457) and *Vibrio cholerae* (MTCC-3906) obtained from Microbial Type Culture Collection (MTCC), Indian Institute of Microbial Technology (IMTECH) Chandigarh were allowed to grow overnight in Luria-Bertani (LB) broth at 37 °C. After appropriate sub-culturing, exponential cultures were swabbed onto freshly prepared LB agar plates and sterile disk (6 mm) were placed on to the plate. The disks were loaded with 20 μl of precursor and complex (1-4) at different concentration (such as 0, 250, 500, 750 and 1000 μg mL⁻¹) along with standard reference drug (Ciprofloxacin). Further, the plates were incubated at 37 °C for 24 h followed by measuring relative

zone of inhibition using a vernier caliper. The experiments were performed in triplicates.

CONCLUSIONS

In this work, surfactant–cobalt(III) complexes (**1–4**) with alkylamine ligands differing in their chain length and number of chain have been synthesized to investigate their tail effect on the hydrophobicity, CMC behaviour, protein interaction and antibacterial activities. On increasing hydrophobicity of surfactant–cobalt(III) complexes (**1–4**), self-assembled micellar size became spherical to rod like morphology, whereas their size distribution gradually increased. It is generally noted a series, **1**→**2**→**3**→**4**, in which CMC values have been decreased, whereas hydrophobicity, protein quenching and binding parameters were increased, indicating that these observation were greatly influenced by the effect of more number of alkylamine ligands compared to that of change in the chain length of alkylamine ligand. Further, it is noted that the thermodynamics of micelles formation is a spontaneous, exothermic and entropy driven process. The temperature dependent interaction of surfactant–cobalt(III) complexes with serum albumins have resulted that the probable quenching mechanism is static and this was further confirmed from ground state protein–complex formation in the UV–Vis studies. On increasing temperature, the protein–complex stability from binding constant values was decreased in the case of single chain system, whereas those were increased in the case of double chain system. This was further confirmed from the thermodynamics of protein interaction, indicating that single chain system is likely to involve in electrostatic interaction ($-\Delta G$, $-\Delta H$ and $+\Delta S$), whereas double chain system is likely to involve in hydrophobic interaction ($-\Delta G$, $+\Delta H$ and $+\Delta S$). Similarly, synchronous fluorescence studies have resulted that the polarity around Trp residues were increased in single chain system due to existence of electrostatic nature, whereas those were decreased in double chain system due to hydrophobic nature. Moreover, CD studies were ensued some appreciable conformational and micro environmental changes in the protein. Furthermore, the complexes **1–4** were more strongly interacted with BSA compared to HSA. It is interesting to visualize that, double chain system possess remarkable antibacterial activity as compared to single chain system. This could be possibly achieved due to the hydrophobic nature of compound that can be easily penetrating the cell membrane. Significantly, this work deals with the tail tune effect which is important for designing the surfactant based metallodrugs, having desired binding mode with drug carrier serum albumins. This kind of tuning the hydrophobicity of surfactant metal complexes with suitable tail ligand could be the better pathway for optimizing the condition for effective biological drugs in near future.

ACKNOWLEDGEMENTS

The authors are grateful to the UGC-SAP & COSIST and DST-FIST programmes of the Department of Chemistry, Bharathidasan University. S.V acknowledges the UGC-RFSMS for financial support as Junior Research Fellowship. SA thanks the sanction of research schemes from funding agencies, CSIR [Grant No. 01(2461)/11/EMR-II] and UGC [Grant No. 41-223/2012(SR)]. The authors thanks to Dr. K. Jeganathan, Co-ordinator, and T.S. Sheena, Research Scholar, Center for NanoScience and Nanotechnology, Bharathidasan University for providing the DLS Measurements. The authors thanks to Dr.P.

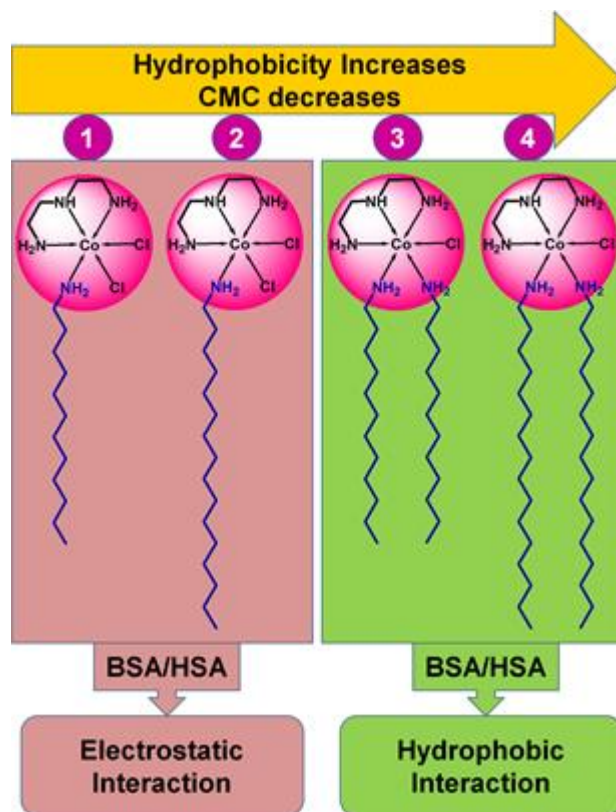
Suresh and Prof.K. Pitchumani, School of chemistry, Madurai Kamaraj University for providing the ESI–MS Measurements.

REFERENCES

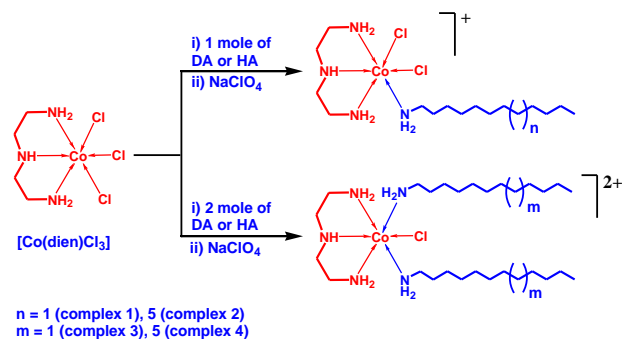
1. X. Zhao, F. Sheng, J. Zheng and R. Liu, *Journal of agricultural and food chemistry*, 2011, 59, 7902-7909.
2. R. Hovland, C. Gløggård, A. J. Aasen and J. Klaveness, *Organic & biomolecular chemistry*, 2003, 1, 644-647.
3. R. W. Storrs, F. D. Tropper, H. Y. Li, C. K. Song, J. K. Kuniyoshi, D. A. Sipkins, K. C. Li and M. D. Bednarski, *Journal of the American Chemical Society*, 1995, 117, 7301-7306.
4. H. Jervis, D. Bruce, M. Raimondi and J. Seddon, *Chemical Communications*, 1999, 2031-2032.
5. E. Kimura, H. Hashimoto and T. Koike, *Journal of the American Chemical Society*, 1996, 118, 10963-10970.
6. G. W. Walker, R. J. Geue, A. M. Sargeson and C. A. Behm, *Dalton Transactions*, 2003, 2992-3001.
7. J. G. Weijnen, A. Koudijs and J. F. Engbersen, *The Journal of Organic Chemistry*, 1992, 57, 7258-7265.
8. G. Ghirlanda, P. Scrimin, A. E. Kaifer and L. A. Echegoyen, *Langmuir*, 1996, 12, 3695-3701.
9. P. n. Řezáčová, J. Pokorná, J. i. Brynda, M. Kožíšek, P. Cígler, M. Lepšík, J. Fanfrlík, J. Rezac, K. r. Grantz Šásková and I. Siegllová, *Journal of medicinal chemistry*, 2009, 52, 7132-7141.
10. M. D. Hall, T. W. Failes, N. Yamamoto and T. W. Hambley, *Dalton Transactions*, 2007, 3983-3990.
11. M. Kožíšek, P. Cígler, M. Lepšík, J. i. Fanfrlík, P. n. Řezáčová, J. i. Brynda, J. Pokorná, J. r. Plešek, B. r. Grüner and K. r. Grantz Šásková, *Journal of medicinal chemistry*, 2008, 51, 4839-4843.
12. C. Zhang, S. Liu, Q. Zhu and Y. Zhou, *Journal of medicinal chemistry*, 2005, 48, 2325-2335.
13. T. Singh, P. Bharmoria, M.-a. Morikawa, N. Kimizuka and A. Kumar, *The Journal of Physical Chemistry B*, 2012, 116, 11924-11935.
14. F. Dimiza, A. N. Papadopoulos, V. Tangoulis, V. Psycharis, C. P. Raptopoulou, D. P. Kessissoglou and G. Psomas, *Dalton Transactions*, 2010, 39, 4517-4528.
15. K. Y. Zhang, S. P.-Y. Li, N. Zhu, I. W.-S. Or, M. S.-H. Cheung, Y.-W. Lam and K. K.-W. Lo, *Inorganic chemistry*, 2010, 49, 2530-2540.
16. S. Nehru, S. Arunachalam, R. Arun and K. Premkumar, *Journal of Biomolecular Structure and Dynamics*, 2013, DOI: 10.1080/07391102.2013.836460, 1-13.
17. R. S. Kumar, S. Arunachalam, V. Periasamy, C. Preethy, A. Riyasdeen and M. Akbarsha, *Journal of inorganic biochemistry*, 2009, 103, 117-127.
18. X. Wu, Y. Tian, M. Yu, J. Han and S. Han, *Biomaterials Science*, 2014.
19. J. Yan, Z. Ye, H. Luo, M. Chen, Y. Zhou, W. Tan, Y. Xiao, Y. Zhang and M. Lang, *Polymer Chemistry*, 2011, 2, 1331-1340.
20. T. Chang, M. Lord, B. Bergmann, A. Macmillan and M. H. Stenzel, *Journal of Materials Chemistry B*, 2014.

21. X. Zhong, J. Guo, L. Feng, X. Xu and D. Zhu, *Colloids and Surfaces A: Physicochemical and Engineering Aspects*, 2014, 441, 572-580.
22. S. Jagadeesan, V. Balasubramanian, P. Baumann, M. Neuburger, D. Häussinger and C. G. Palivan, *Inorganic chemistry*, 2013.
23. N. Kumaraguru and K. Santhakumar, *Physics and Chemistry of Liquids*, 2010, 48, 747-763.
24. K. Santhakumar, N. Kumaraguru, M. Arumugham and S. Arunachalam, *Polyhedron*, 2006, 25, 1507-1513.
25. P. Mukerjee, *The Journal of Physical Chemistry*, 1962, 66, 1375-1376.
26. O. Owoyomi, J. Ige and O. Soriyan, *Chemical Sciences Journal*, 2011, 2011.
27. Y. Ni, R. Zhu and S. Kokot, *Analyst*, 2011, 136, 4794-4801.
28. X.-X. Cheng, Y. Lui, B. Zhou, X.-H. Xiao and Y. Liu, *Spectrochimica Acta Part A: Molecular and Biomolecular Spectroscopy*, 2009, 72, 922-928.
29. C.-Q. Xiao, F.-L. Jiang, B. Zhou, R. Li and Y. Liu, *Photochemical & Photobiological Sciences*, 2011, 10, 1110-1117.
30. F. Samari, B. Hemmateenejad, M. Shamsipur, M. Rashidi and H. Samouei, *Inorganic chemistry*, 2012, 51, 3454-3464.
31. C.-Y. Yang, Y. Liu, D. Zheng, J.-C. Zhu and J. Dai, *Journal of Photochemistry and Photobiology A: Chemistry*, 2007, 188, 51-55.
32. D. Shcharbin, E. Pedziwiatr, L. Chonco, J. F. Bermejo-Martín, P. Ortega, F. J. de la Mata, R. Eritja, R. Gómez, B. Klajnert and M. Bryszewska, *Biomacromolecules*, 2007, 8, 2059-2062.
33. P. D. Ross and S. Subramanian, *Biochemistry*, 1981, 20, 3096-3102.
34. M. Yu, Z. Ding, F. Jiang, X. Ding, J. Sun, S. Chen and G. Lv, *Spectrochimica Acta Part A: Molecular and Biomolecular Spectroscopy*, 2011, 83, 453-460.
35. B. K. Paul, A. Samanta and N. Guchhait, *The Journal of Physical Chemistry B*, 2010, 114, 6183-6196.
36. Q. Yang, J. Liang and H. Han, *The Journal of Physical Chemistry B*, 2009, 113, 10454-10458.
37. Z. Chi, R. Liu, Y. Teng, X. Fang and C. Gao, *Journal of agricultural and food chemistry*, 2010, 58, 10262-10269.
38. R. S. Kumar and S. Arunachalam, *Biophysical chemistry*, 2008, 136, 136-144.
39. A. Colomer, A. Pinazo, M. Manresa, M. Vinardell, M. Mitjans, M. Infante and L. Pérez, *Journal of medicinal chemistry*, 2011, 54, 989-1002.
40. R. Kitson, *Analytical Chemistry*, 1950, 22, 664-667.
41. S. H. Caldwell and D. House, *Journal of Inorganic and Nuclear Chemistry*, 1969, 31, 811-823.
42. R. K. Gupta, R. Pandey, G. Sharma, R. Prasad, B. Koch, S. Srikrishna, P.-Z. Li, Q. Xu and D. S. Pandey, *Inorganic chemistry*, 2013, 52, 3687-3698.
43. A. Gonzalez-Perez, J. Del Castillo, J. Czapkiewicz and J. Rodríguez, *Colloid and Polymer Science*, 2002, 280, 503-508.
44. R. Zana, *Journal of Colloid and Interface Science*, 1980, 78, 330-337.
45. M. Van De Weert, *Journal of fluorescence*, 2010, 20, 625-629.
46. J. R. Lakowicz, *Principles of fluorescence spectroscopy*, Springer, 2009.
47. Y.-Z. Zhang, B. Zhou, Y.-X. Liu, C.-X. Zhou, X.-L. Ding and Y. Liu, *Journal of fluorescence*, 2008, 18, 109-118.
48. S. Soares, N. Mateus and V. De Freitas, *Journal of agricultural and food chemistry*, 2007, 55, 6726-6735.
49. A. Tarushi, J. Kljun, I. Turel, A. A. Pantazaki, G. Psomas and D. P. Kessissoglou, *New Journal of Chemistry*, 2013, 37, 342-355.
50. A. Divsalar, M. J. Bagheri, A. A. Saboury, H. Mansoori-Torshizi and M. Amani, *The Journal of Physical Chemistry B*, 2009, 113, 14035-14042.
51. A. Tanwir, R. Jahan, M. A. Quadir, M. A. Kaisar and M. K. Hossain, *Dhaka University Journal of Pharmaceutical Sciences*, 2012, 11, 45-49.
52. J. Zhang, X.-J. Wang, Y.-J. Yan and W.-S. Xiang, *Journal of agricultural and food chemistry*, 2011, 59, 7506-7513.
53. P. Bolel, N. Mahapatra and M. Halder, *Journal of agricultural and food chemistry*, 2012, 60, 3727-3734.
54. J. Mandeville and H. Tajmir-Riahi, *Biomacromolecules*, 2010, 11, 465-472.

Table of Contents



Highlights: Single chain surfactant–cobalt(III) complexes interact with serum albumins electrostatically, whereas double chain surfactant–cobalt(III) complexes interact with serum albumins hydrophobically.



Scheme 1. Schematic representation of synthesis of single and double chain surfactant-cobalt(III) complexes

Table and Figures Captions

Table 1. Critical micelles concentration values and thermodynamic parameters of surfactant–cobalt(III) complexes

Table 2. The Stern–Volmer quenching constant (K_{sv}), quenching rate constant (k_q), binding constant (K_b), binding number (n) and the thermodynamic parameters (ΔH° , ΔG° and ΔS°) for the interaction of surfactant–cobalt(III) complexes with BSA/HAS at different temperatures.

Table 3. Antibacterial effect of surfactant–cobalt(III) complexes at different concentrations

Figure 1. Structural representation of single and double chain surfactant metal complexes

Figure 2. SEM images (a) and Size distribution histogram plots (b) for self–assembled surfactant–cobalt(III) complexes **1–4**

Figure 3. Plots for specific conductivity versus concentration of surfactant–cobalt(III) complexes (**3** and **4**) in aqueous solution

Figure 4. UV–visible absorption spectra of (a) BSA and (b) HSA in the absence and presence of complex **2**. [BSA] = [HSA] = 10 μM and [surfactant–cobalt(III) complex] = 90 μM , pH = 7.4

Figure 5. Plot of % relative fluorescence intensity of (a) BSA ($\lambda_{em} = 350$ nm) and (b) HSA ($\lambda_{em} = 346$ nm) at various concentrations of complexes **1–4** ($r = [\text{complex}]/[\text{BSA or HSA}] = 0\text{--}90$ μM), pH = 7.4

Figure 6. Effect of addition of complexes **1–4** ($R = [\text{complex}]/[\text{BSA or HSA}]$) on the relative synchronous fluorescence intensity of BSA (left, A) and HSA (right, B) at $\Delta\lambda = 15$ nm (top, 1), $\Delta\lambda = 60$ nm (bottom, 2); BSA = HSA = 10 μM and [surfactant–cobalt(III) complex] = 90 μM , pH = 7.4

Figure 7. Circular Dichroism spectra of (a) BSA and (b) HSA in the absence and presence of complexes **1–4**. [BSA] = [HSA] = 2 μM , [surfactant–cobalt(III) complexes] = 4 μM , pH = 7.4

Table 1

Complexes	T (K)	CMC $\times 10^4$ M	ΔG_m° (kJ mol $^{-1}$)	ΔH_m° (kJ mol $^{-1}$)	ΔS_m° (J mol $^{-1}$ K $^{-1}$)
1	303	4.8045	–31.201	–16.704	+49.248
	308	4.9909	–32.068	–17.538	+48.012
	313	5.3667	–33.612	–18.861	+47.128
	318	5.8333	–34.525	–19.903	+45.981
	323	6.2348	–35.290	–20.850	+44.706
	2	303	1.3841	–38.237	–30.121
308		1.6013	–38.251	–31.140	+23.088
313		1.8097	–40.274	–33.792	+20.709
318		1.9918	–41.009	–35.352	+17.789
323		2.2091	–42.166	–37.375	+14.833
3		303	0.6990	–44.629	–6.8109
	308	0.7207	–46.393	–8.0781	+124.39
	313	0.7403	–47.229	–8.6087	+123.38
	318	0.7612	–48.705	–9.5644	+123.08
	323	0.7815	–49.849	–10.711	+121.17
	4	303	0.1598	–52.248	–29.098
308		0.1773	–52.837	–30.196	+73.509
313		0.2023	–53.621	–31.522	+70.603
318		0.2253	–54.159	–32.634	+67.689
323		0.2387	–54.760	–33.737	+65.088

Table 2

Complexes	T(K)	$K_{sv} \times 10^{-4}$ (M ⁻¹)	$k_q \times 10^{-12}$ (M ⁻¹ S ⁻¹)	$K_b \times 10^{-4}$ (M ⁻¹)	n	ΔH° (kJmol ⁻¹)	ΔG° (kJmol ⁻¹)	ΔS° (J mol ⁻¹ K ⁻¹)
BSA-1	278	0.3910	0.3910	1.3728	1.1456	-16.742	-22.020	+19.037
	293	0.4067	0.4067	0.9517	1.0957			
	308	0.4321	0.4321	0.6135	1.0411			
BSA-2	278	0.4905	0.4905	32.569	1.4485	-19.804	-29.339	+34.197
	293	0.5300	0.5300	19.907	1.4062			
	308	0.5736	0.5736	11.604	1.3304			
BSA-3	278	2.4522	2.4522	113.53	1.4387	+8.665	-32.225	+146.997
	293	2.7625	2.7625	134.15	1.4479			
	308	2.9201	2.9201	190.29	1.4541			
BSA-4	278	3.5229	3.5229	247.80	1.4745	+45.696	-34.029	+286.885
	293	4.1973	4.1973	736.55	1.5745			
	308	4.5578	4.5578	105.22	1.6007			
HSA-1	278	0.3616	0.3616	0.2515	0.9601	-11.960	-18.098	+22.188
	293	0.3783	0.3783	0.1986	0.9216			
	308	0.3893	0.3893	0.1408	0.8832			
HSA-2	278	0.5393	0.5393	12.966	1.3147	-14.556	-27.210	+45.688
	293	0.6392	0.6392	7.9305	1.2728			
	308	0.6674	0.6674	4.5930	1.2029			
HSA-3	278	2.5342	2.5342	13.231	1.1921	+42.198	-27.257	+249.599
	293	2.5396	2.5396	32.077	1.2812			
	308	2.7061	2.7061	100.76	1.3971			
HSA-4	278	2.7486	2.7486	100.93	1.2912	+60.996	-31.953	+325.024
	293	2.8539	2.8539	159.88	1.4059			
	308	3.4532	3.4532	655.09	1.5540			

Table 3

Bacterial strain used	Zone of Inhibition (in mm)																				
	Standard	Complex-1 (µg mL ⁻¹)					Complex-2 (µg mL ⁻¹)					Complex-3 (µg mL ⁻¹)					Complex-4 (µg mL ⁻¹)				
	(µg mL ⁻¹)	1000	0	250	500	750	1000	0	250	500	750	1000	0	250	500	750	1000	0	250	500	750
<i>E. coli</i>	28	0	10.5	13	14.5	17	0	12	14.5	16	17	0	12	13.5	15	17	0	10.5	13.5	15	18.5
<i>K. pneumoniae</i>	21	0	10	11.5	11	13	0	9.5	10.5	12	14	0	11.5	13	14	17	0	10.5	12	14	14
<i>P. aeruginosa</i>	20	0	8.5	10.5	11	12	0	12	12.5	13	15	0	8.5	10.5	13	15	0	11.5	12	12.5	14
<i>P. vulgaris</i>	26	0	8	11.5	12.5	13.5	0	9.5	10.5	12	14	0	9.5	11	12	13.5	0	10.5	14.5	15.5	17
<i>S. typhi</i>	26	0	10	11	12	13	0	8.5	11	13	15	0	10.5	12.5	11.5	15.5	0	9.5	12.5	14	15.5
<i>S. flexneri</i>	25	0	10	11.5	11	13	0	9.5	10.5	12	14	0	11.5	12.5	14.5	15	0	12	13	14.5	16
<i>S. aureus</i>	26	0	8.5	11.5	12.5	13.5	0	10.5	14	16	17	0	13.5	16	16	17	0	12.5	14	14.5	17
<i>V. cholerae</i>	22	0	7	9	10.5	11.5	0	10.5	13	13	15	0	9	9.5	11	13.5	0	12	13	14.5	16

Standard – Ciprofloxacin

Solvent – Water (Showed nil effect against the microorganisms under test).

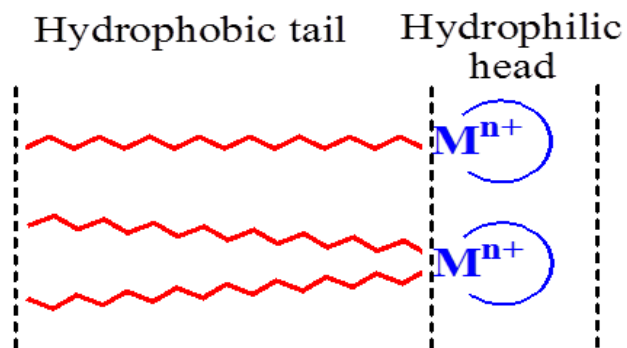


Figure 1

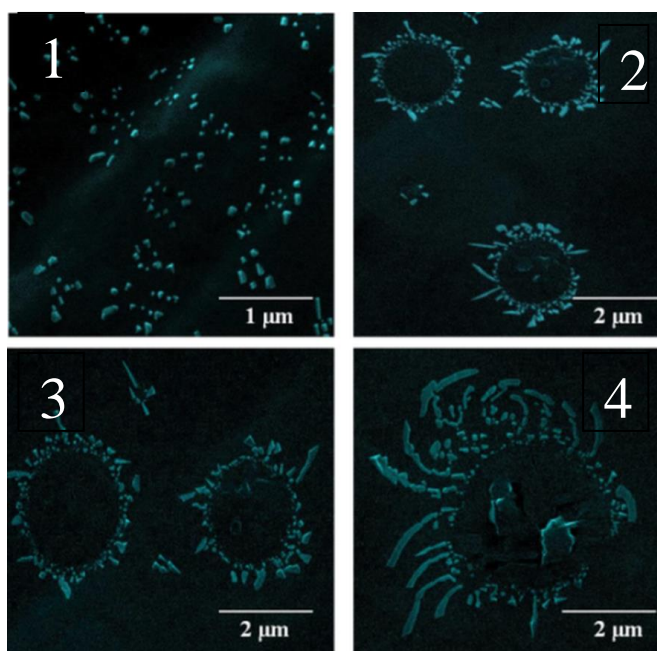


Figure 2(a)

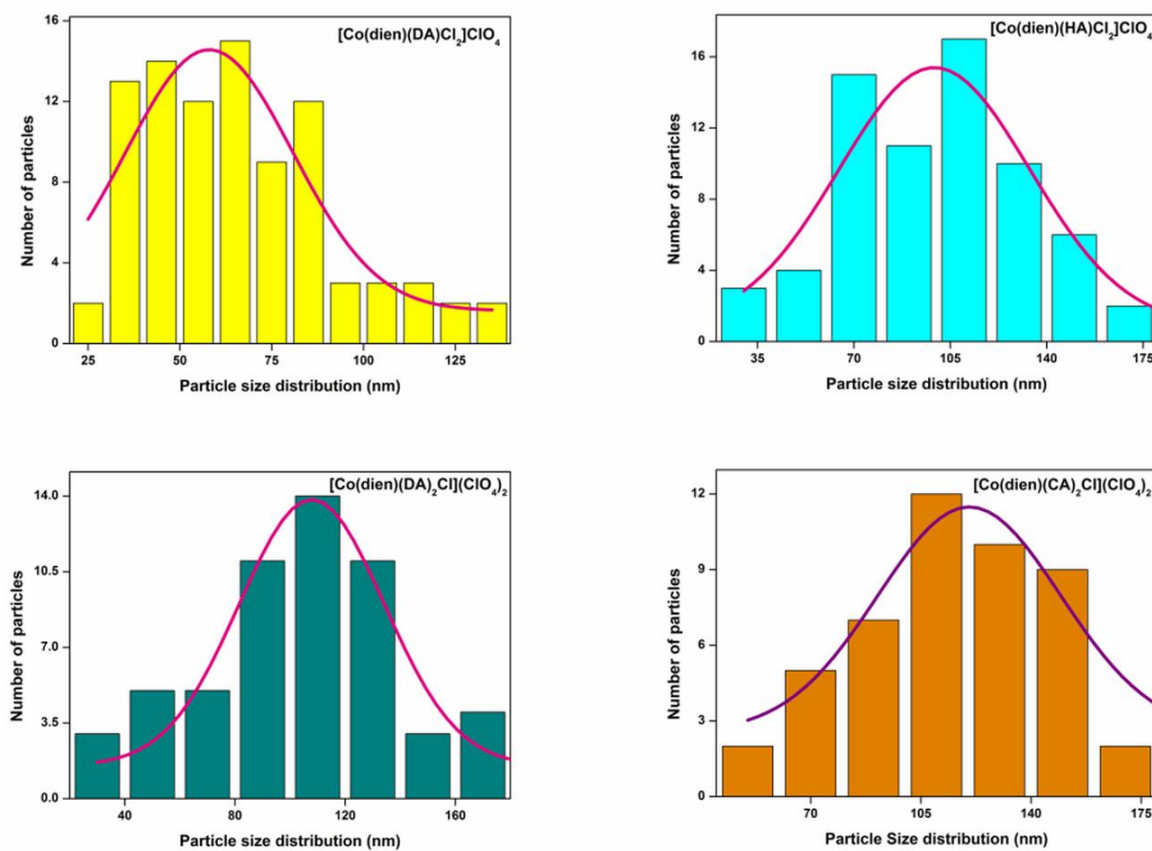


Figure 2(b)

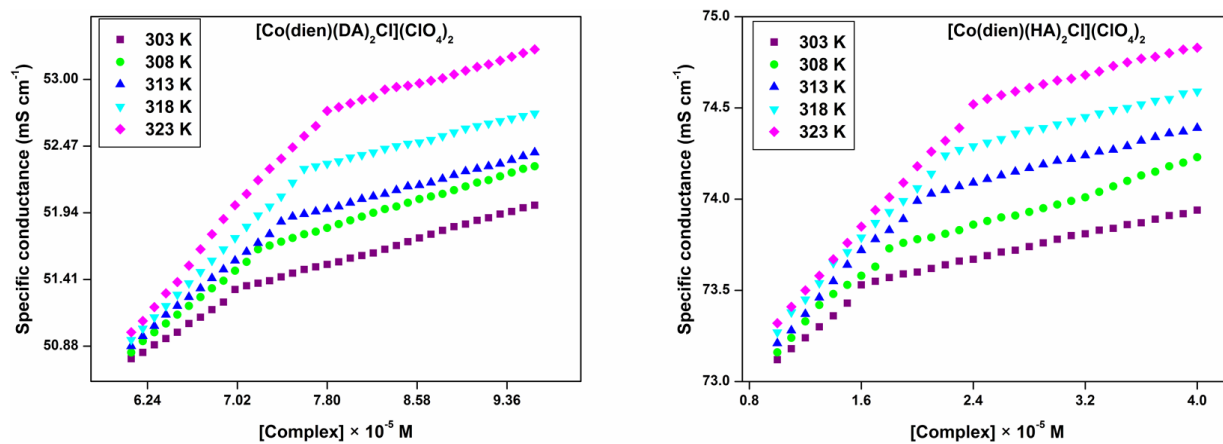


Figure 3

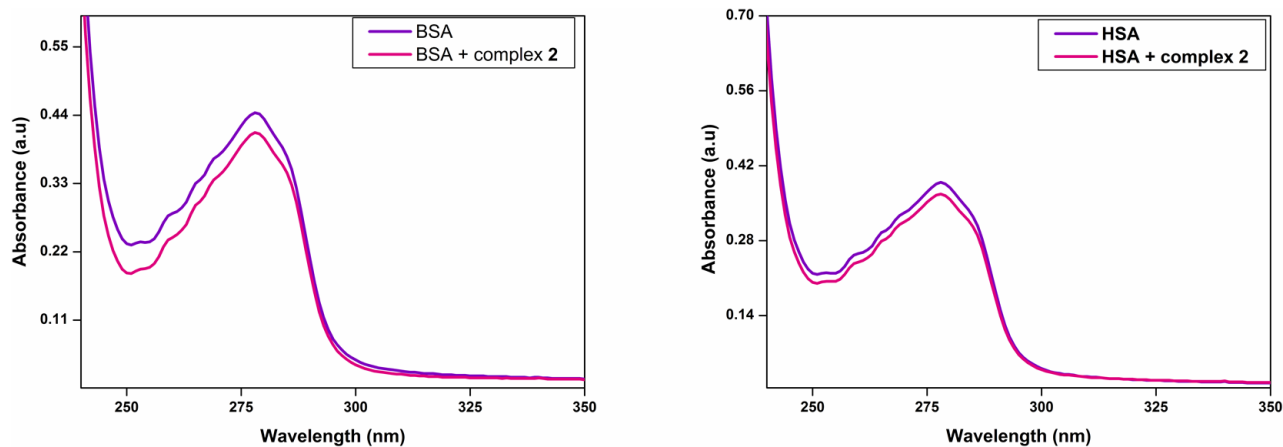


Figure 4

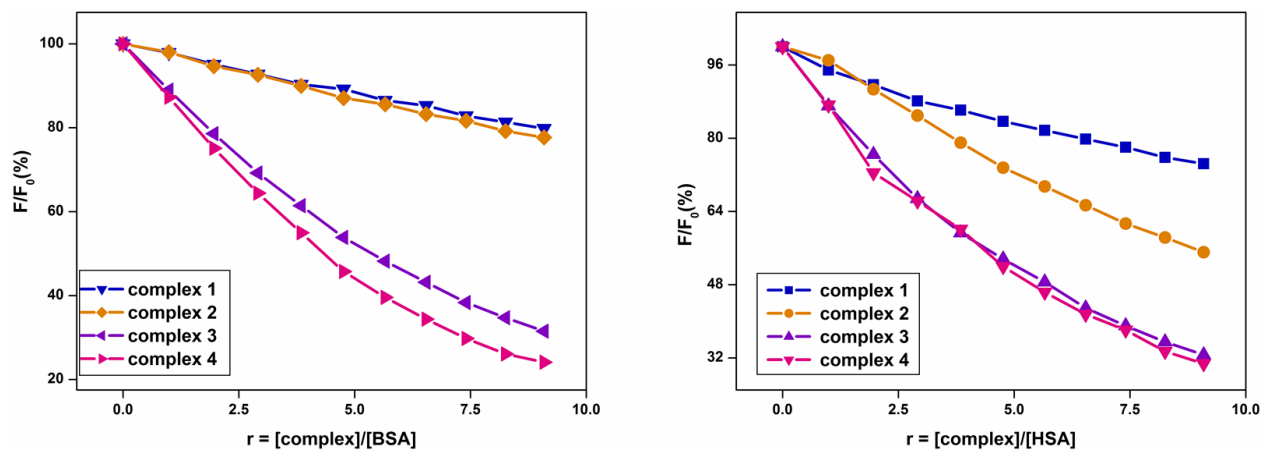


Figure 5

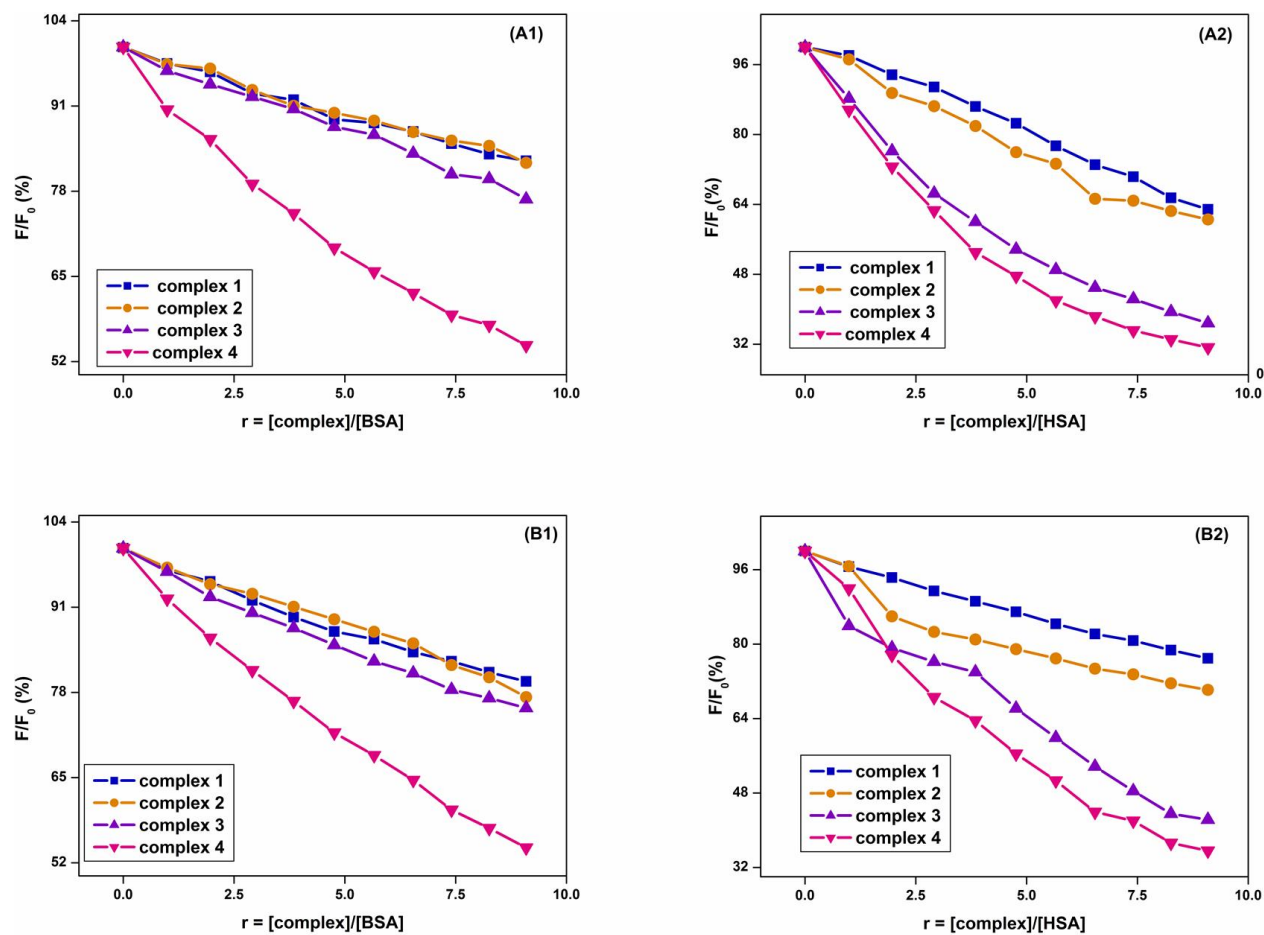


Figure 6

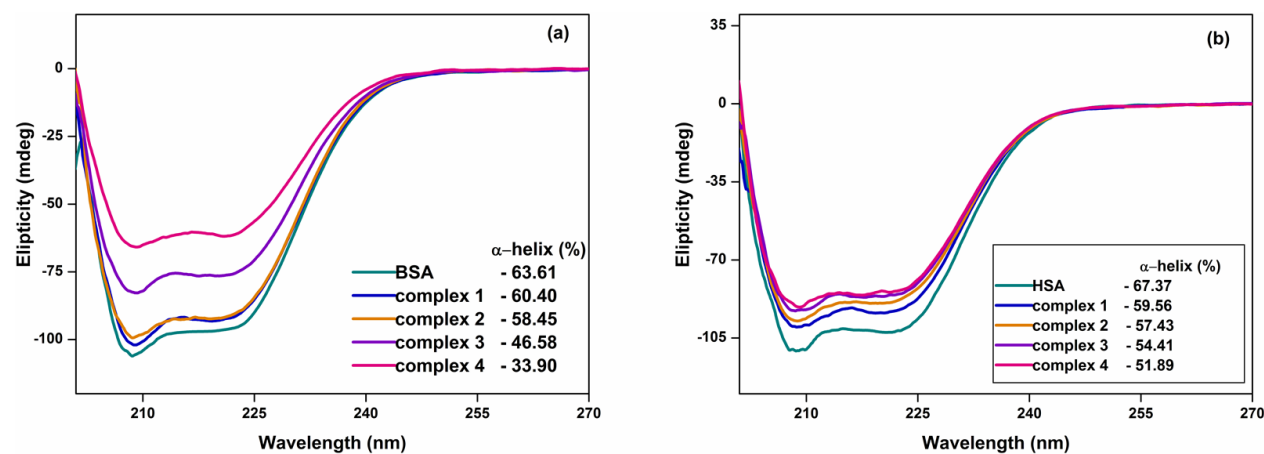


Figure 7